APPLIED PHYSICS LETTERS **90**, 253108 (2007)

Charge storage characteristics of atomic layer deposited RuO_x nanocrystals

S. Maikap[a)]
Department of Electronic Engineering, Chang Gung University, Tao-Yuan, Taiwan 333, Republic of China

T. Y. Wang
Department of Material Science Engineering, National Taiwan University, Taipei, Taiwan 106, Republic of China

P. J. Tzeng, C. H. Lin, and L. S. Lee
Electronic and Opto-electronic Research Laboratories, Industrial Technology Research Institute, Hsinchu, Taiwan 310, Republic of China

J. R. Yang
Department of Material Science Engineering, National Taiwan University, Taipei, Taiwan 106, Republic of China

M. J. Tsai
Electronic and Optoelectronic Research Laboratories, Industrial Technology Research Institute, Hsinchu, Taiwan 310, Republic of China

(Received 2 April 2007; accepted 24 May 2007; published online 19 June 2007)

The charge storage characteristics of atomic layer deposited RuO_x nanocrystals embedded in high-*k* HfO_2/Al_2O_3 films in a metal/$Al_2O_3/RuO_x/HfO_2/SiO_2/n$-Si structure have been investigated. The size and density of RuO_x nanocrystals have been measured using transmission electron microscopy. The RuO_x nanocrystals show a density of $\sim 1\times 10^{12}/\text{cm}^2$ and a diameter of 5–8 nm. A large hysteresis memory window of ~13.3 V at a gate voltage of 9 V has been observed for RuO_x nanocrystal memory capacitors. A hysteresis memory window of 0.7 V has also been observed under a small sweeping gate voltage of 1 V. A promising memory window of RuO_x nanocrystals has been observed as compared with those of pure HfO_2 and Al_2O_3 charge trapping layers, due to charge storage in the RuO_x metal nanocrystals. The RuO_x nanocrystal memory capacitor has similar leakage current with the pure HfO_2 and Al_2O_3 charge trapping layers. The RuO_x memory capacitor has a large breakdown voltage of ~13.8 V. © *2007 American Institute of Physics*.
[DOI: 10.1063/1.2749857]

Nonvolatile memory devices with a low gate voltage operation, consuming less power and allowing higher integration with high-speed writing and erasing of data have an important role in semiconductor industry for future nanoscale flash memory device applications. Silicon nitride (Si_3N_4) charge trapping layers in a polycrystalline-silicon–oxide–silicon-nitride–oxide–silicon (SONOS) structure with poor retention and scaling problem have been reported.[1] The nonvolatile memory devices with high-*k* charge trapping layers in SONOS structure have been reported by several researchers.[2–5] To improve the device performance, memory device structures with nanocrystals (or quantum dots) have been reported for the possible solution of next generation of nonvolatile memory device applications.[6–21] However, for the integration of nanocrystals into the memory device structure, it is a challenging task to control the highly reproducible memory device with a high spatial density, small size, and narrow size distribution of the nanocrystals. Recently, the memory structure with ruthenium (Ru) nanocrystals has also been reported.[17] To get high density, small size, and narrow size distribution of nanocrystals, the memory devices with metal nanocrystals formed by atomic layer deposition (ALD) have not yet been reported. In this letter, the memory device structure with ruthenium oxide (RuO_x) nanocrystals formed by atomic layer deposition has been investigated. The RuO_x is an attractive candidate for metal nanocrystal memories because it has a large work function of ~4.8 eV to bring about deep quantum well. Furthermore, high-*k* materials with a large barrier height, such as Al_2O_3 film, are interesting alternatives as a blocking oxide to improve the device performance and scaling. A large memory window with a low gate voltage ($V_g < 5$ V), small size (5–8 nm), high density ($\sim 1\times 10^{12}/\text{cm}^2$), and good uniformity have been observed for atomic layer deposited RuO_x nanocrystals in a platinum/$Al_2O_3/RuO_x/HfO_2/SiO_2/n$-Si structure for nanoscale high-performance flash memory device applications. The pure HfO_2 and Al_2O_3 charge trapping memory devices have also been fabricated for comparison.

N-type Si (100) substrate with a resistivity of ~1 Ohm-cm was cleaned by the RCA process to remove native oxide from the surface. After cleaning the *n*-type Si substrate, a tunneling oxide (SiO_2) with a thickness of 3 nm was grown by rapid thermal oxidation system at 1000 °C for 15 s. The high-*k* HfO_2 film as a wetting layer was grown by ALD using hafnium tetrachloride ($HfCl_4$) precursor at a substrate temperature of 300 °C. The thickness of HfO_2 film was ~2 nm. Then, the ruthenium oxide (RuO_x) layer with a thickness of ~2 nm was grown by ALD using diethylcyclopentadienyl ruthenium [$Ru(EtCp)_2$] precursor at a substrate temperature of 350 °C. Then, the high-*k* Al_2O_3 film as a blocking oxide was grown by ALD using trimethylalu-

---

[a)] Author to whom correspondence should be addressed; electronic mail: sidhu@mail.cgu.edu.tw

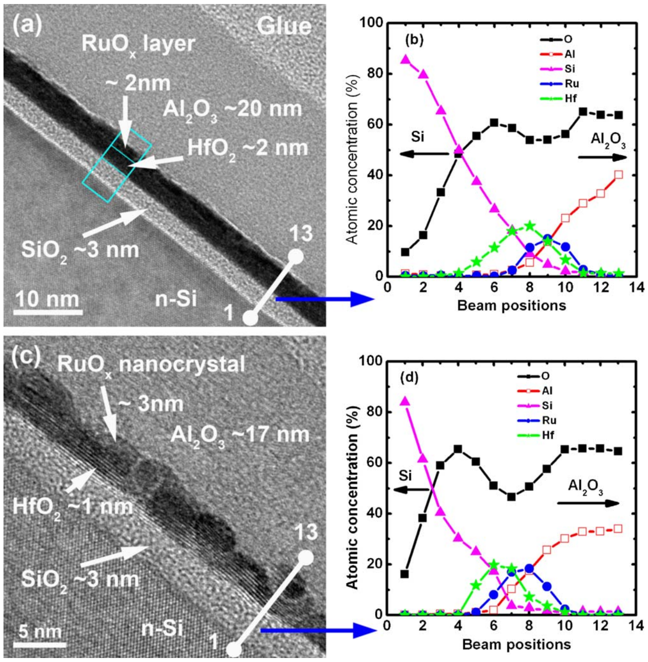

FIG. 1. (Color online) High-resolution transmission electron microscopy (TEM) images of $Al_2O_3/RuO_x/HfO_2/SiO_2/n$-Si structure for (a) as-deposited and (c) 900 °C, 1 min samples. Average elemental concentrations of oxygen (O), silicon (Si), hafnium (Hf), ruthenium (Ru), and aluminum (Al) for the (b) as-deposited and (d) annealed samples have been shown. Clear RuO_x metal nanocrystals have been observed for annealed sample.

minum $[Al(CH_3)_3]$ precursor at a substrate temperature of 300 °C. The H_2O precursor was used for oxygen. The thickness of Al_2O_3 film was ~20 nm. The precursor temperatures were 185 °C for $HfCl_4$, 100 °C for $Ru(EtCp)_2$ and 23 °C for $Al(CH_3)_3$. Due to an unoptimized process, the oxygen can be included into the Ru film, resulting in a RuO_x layer, by ALD. To form the RuO_x nanocrystals, a postdeposition annealing (PDA) treatment at a temperature of 900 °C for 1 min was performed in N_2 (90%) and O_2 (10%) gases. The platinum (Pt) metal gate electrode (gate area: 1.12×10^{-4} cm^2) was used for all memory capacitors. The postmetal annealing was performed with a temperature of 400 °C for 5 min in N_2 (90%) and H_2 (10%) gases. To investigate the charge storage characteristics, the memory capacitor structures were designed such as S1: n-$Si/SiO_2(3\text{ nm})/Al_2O_3(20\text{ nm})/Pt$, S2: n-$Si/SiO_2(3\text{ nm})/HfO_2(2\text{ nm})/Al_2O_3(20\text{ nm})/Pt$, and S3: n-$Si/SiO_2(3\text{ nm})/HfO_2(2\text{ nm})/RuO_x(2\text{ nm})/Al_2O_3(20\text{ nm})/Pt$. The memory capacitors (S1 and S2) were fabricated for comparison. To probe the size and microstructure of RuO_x nanocrystals, high-resolution transmission electron microscopy was carried out using a FEI Tecnai F30 field emission system with an operating voltage of 300 kV and a resolution of 0.17 nm. Electrical characteristics of all memory capacitors were performed using a HP 4284A *LCR* meter and HP4156B semiconductor analyzer systems.

Figures 1(a) and 1(c) show the cross-sectional TEM images of the n-$Si/SiO_2/HfO_2/RuO_x/Al_2O_3$ (sample: S3) structure for as deposited and after PDA treatment, respectively. The thicknesses of SiO_2, HfO_2, RuO_x, and Al_2O_3 films are found to be 3.0, 2.0, 2.0, and 20 nm, respectively, for the as-deposited sample. The HfO_2 and RuO_x films show partial crystallinity while the Al_2O_3 film shows amorphous nature. After the annealing treatment, clear RuO_x nanocrystals embedded in HfO_2 and Al_2O_3 films have been observed.

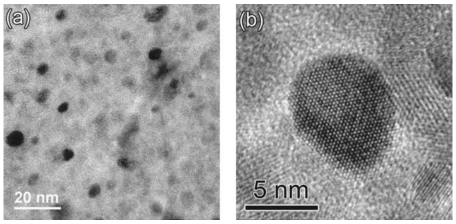

FIG. 2. (a) Plan-view transmission electron microscopy image of RuO_x nanocrystals in $Al_2O_3/RuO_x/HfO_2/SiO_2/n$-Si structure and (b) high-resolution TEM image of a single RuO_2 nanocrystal.

The average diameter of RuO_x nanocrystals is 5–8 nm and the thickness is about 3 nm. The thicknesses of SiO_2, HfO_2, and Al_2O_3 films are found to be 3.0, 1.0, and 17 nm, respectively. The lattice constants of Ru film (hexagonal) are calculated: $a=0.275$ nm, $b=0.275$ nm, $c=0.443$ nm. The lattice constants of monoclinic HfO_2 films are found to be $a=0.511$ nm, $b=0.517$ nm, and $c=0.529$ nm, while those values are found to be $a=0.448$ nm, $b=0.443$ nm, and $c=0.309$ nm for the orthorhombic RuO_2 films. Note that the HfO_2 film as a wetting layer has been used because the RuO_x film cannot be directly deposited by ALD on SiO_2 without HfO_2 film. The reason for RuO_x film deposition on HfO_2 layers is unclear. It is also beneficial that the high-HfO_2 layer can be used as a part of tunneling oxide.

The elemental compositions of n-$Si/SiO_2/HfO_2/RuO_x/Al_2O_3$ (sample: S3) structure were investigated by energy dispersive x-ray spectroscopy (EDS) analysis with a spot size of ~0.5 nm and a spatial resolution of ~1 nm. Figures 1(b) and 1(d) show the elemental concentrations of O, Hf, Si, Ru, and Al measured by EDS for the as deposited and after annealing treatment. The numbers indicated on the curve in Figs. 1(b) and 1(d) correspond to the numbers shown in the TEM image. It is estimated that the SiO_2, HfO_2, and Al_2O_3 films show close stoichiometric for the as-deposited and annealing treated samples. Average concentrations of Hf, Ru, and O atoms are found to be 20, 14, and 54 at. %, respectively, for the as-deposited sample, while those values are found to be 20, 18, and 47 at. %, respectively, for the annealed sample. After annealing treatment, it is shown that the Ru-rich RuO_x nanocrystal is formed in our memory structure. The high density of $\sim1\times10^{12}/\text{cm}^2$ for RuO_x nanocrystals measured by plan-view TEM is observed (Fig. 2). The diameter of nanocrystals is 5–8 nm. The thickness of nanocrystal is about 3 nm. It indicates that the shape of nanocrystal is likely a thick disk. The density and size of RuO_x nanocrystals can be controlled by changing the thickness of the RuO_x layer.

Figure 3(a) shows a good clockwise hysteresis of RuO_x nanocrystal memory capacitors with different sweeping gate voltages (V_g). A small capacitance equivalent thickness is found to be ~9.3 nm. The high-frequency (1 MHz) capacitance-voltage (*C-V*) has been measured with a hold time of 100 ms. A large hysteresis memory window of 13.3 V at sweeping gate voltage of $V_g=9$ V is observed, due to the high density of RuO_x metal nanocrystals. Yim *et al.*[17] reported the hysteresis memory window of ~6.7 V at a large sweeping gate voltage of 10 V for Ru nanocrystal memory device. A hysteresis memory window of ~0.7 V is also observed under an extremely low gate voltage of ±1 V, due to deep quantum well (high work function of ~4.8 eV) of RuO_x nanocrystals and small conduction band offset

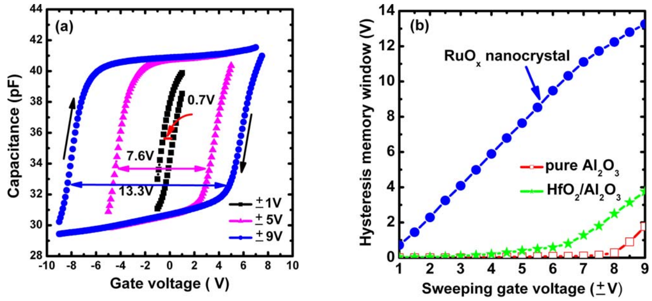

FIG. 3. (Color online) (a) Capacitance vs sweeping gate voltage characteristics of RuO$_x$ nanocrystal memory capacitors. (b) The hysteresis memory window increases with increasing the sweeping gate voltage.

($\Delta E_c \sim 1.7$ eV) of HfO$_2$ films. It indicates that the charge can be stored in the RuO$_x$ nanocrystals under small positive gate voltage and the stored charges can be erased easily under small negative gate voltage applications. The RuO$_x$ metal nanocrystal memory devices formed by ALD show the best hysteresis memory characteristics as compared with reported nanocrystal memory devices in the literatures.[17,18] The amount of stored charges in RuO$_x$ nanocrystals can be estimated using the relation $Q = C_{\mathrm{ox}} x (+V_{\mathrm{FB}})$, where C_{ox} ($\approx 3.7 \times 10^{-7}$ F/cm^2) is the capacitance density at accumulation region and $+V_{\mathrm{FB}}$ (≈ 4.4 V) is the flatband voltage shift under a positive gate voltage of $V_g \approx 6$ V. Thus, the electron density stored in RuO$_x$ nanocrystals is estimated to be $\sim 1 \times 10^{13}$/cm^2. It indicates that one RuO$_x$ nanocrystal can store about ten electrons, which is similar to the reported results on HfO$_2$ nanocrystals.[11] The hysteresis memory window of RuO$_x$ nanocrystal capacitor increases with an increase of the sweeping gate voltage up to 9 V [Fig. 3(b)]. The nanocrystal capacitor has a large hysteresis memory window as compared with those of the pure HfO$_2$ and Al$_2$O$_3$ charge trapping layers. Large memory windows with a low gate voltage operation of RuO$_x$ nanocrystal memory capacitor can be used in future nanoscale flash memory device applications.

The leakage current density of RuO$_x$ nanocrystal capacitor is similar to those of the pure HfO$_2$ and Al$_2$O$_3$ charge trapping layers up to a gate voltage of 9 V (Fig. 4). The RuO$_x$ nanocrystal capacitor shows the breakdown voltage of −13.8 V and leakage current density of 5×10^{-10} A/cm^2 at a gate voltage of −5 V. A breakdown voltage (−13.8 V) of RuO$_x$ nanocrystal is lower (slightly) as compared with that of the breakdown voltage of 17 V for pure HfO$_2$ charge trapping layer, and it may be due to the contamination (slight) of RuO$_x$ metals in the Al$_2$O$_3$ blocking oxide after annealing treatment.

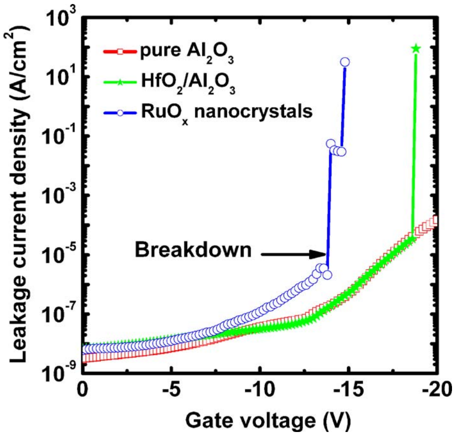

FIG. 4. (Color online) Leakage current densities of RuO$_x$ nanocrystal, pure HfO$_2$, and Al$_2$O$_3$ charge trapping layers.

In conclusion, the excellent charge storage characteristics of atomic layer deposited RuO$_x$ nanocrystal capacitors have been observed. A large hysteresis memory window of 13.3 V at a sweeping gate voltage of 9 V, low leakage current density of 5×10^{-10}/cm^2 at a gate voltage of −5 V, and high breakdown voltage of −13.8 V have been investigated. The atomic layer deposited RuO$_x$ nanocrystal memory capacitor can be used in future nanoscale high-speed flash memory device applications.

[1] J. R. Hwang, T. L. Lee, H. C. Ma, T. C. Lee, T. H. Chung, C. Y. Chang, S. D. Liu, B. C. Perng, J. W. Hsu, M. Y. Lee, C. Y. Ting, C.-C. Huang, J. H. Shieh, and F.-L. Yang, Tech. Dig. - Int. Electron Devices Meet. **2005**, 161.

[2] Y. N. Tan, W. K. Chim, B. J. Cho, and W. K. Choi, IEEE Trans. Electron Devices **51**, 1143 (2004).

[3] S. Maikap, P.-J. Tzeng, L. S. Lee, H. Y. Lee, C. C. Wang, P. H. Tsai, K. S. Chang-Liao, W. J. Chen, K. C. Liu, P. R. Jeng, and M. J. Tsai, Proceedings of the 2006 International Symposium on VLSI Technology, Systems, and Applications, 2006 (unpublished), p. 36.

[4] M. S. Joo, S. R. Lee, H. Yang, K. Hong, S.-A. Jang, J. Koo, J. Kim, S. Shin, M. Kim, S. Pyi, N. Kwak, and J.-W. Kim, Extended Abstract of the 2006 International Conference on Solid State Devices and Materials (unpublished), p. 982.

[5] S. Maikap, P. J. Tzeng, T. Y. Wang, H. Y. Lee, C. H. Lin, C. C. Wang, L. S. Lee, J. R. Yang, and M. J. Tsai, Jpn. J. Appl. Phys., Part 1 **46** 1803 (2007).

[6] S. Tiwari, F. Rana, K. Chan, L. Shi, and H. Hanafi, Appl. Phys. Lett. **69**, 1232 (1996).

[7] T. Z. Lu, M. Alexe, R. Scholz, V. Talelaev, and M. Zacharias, Appl. Phys. Lett. **87**, 202110 (2005).

[8] J. Brault, M. Saitoh, and T. Hiramoto, IEEE Trans. Nanotechnol. **4**, 349 (2005).

[9] K. Das, M. NandaGoswami, R. Mahapatra, G. S. Kar, A. Dhar, H. N. Acharya, S. Maikap, J. H. Lee, and S. K. Ray, Appl. Phys. Lett. **84**, 1386 (2004).

[10] T. H. Ng, W. K. Chim, and W. K. Choi, Appl. Phys. Lett. **88**, 113112 (2006).

[11] Y. H. Lin, C. H. Chien, C. T. Lin, C. Y. Chang, and T. F. Lei, IEEE Trans. Electron Devices **53**, 782 (2006).

[12] H.-C. You, T.-H. Hsu, F.-H. Ko, J.-W. Huang, and T.-F. Lei, IEEE Electron Device Lett. **27**, 644 (2006).

[13] Z. Liu, C. Lee, V. Narayanan, G. Pei, and E. C. Kan, IEEE Trans. Electron Devices **49**, 1606 (2002).

[14] J. J. Lee, Y. Harada, J. W. Pyun, and D. L. Kwong, Appl. Phys. Lett. **86**, 102505 (2005).

[15] S. K. Samanta, W. J. Yoo, G. Samudra, E. S. Tok, L. K. Bera, and N. Balasubramanian, Appl. Phys. Lett. **87**, 113110 (2005).

[16] S.-H. Lim, K. H. Joo, J.-H. Park, S.-W. Lee, W. H. Sohn, C. Lee, G. H. Choi, I.-S. Yeo, U.-I. Chung, J. T. Moon, and B.-I. Ryu, 2005 Symposium on VLSI Technology, Digest of Technical Papers (unpublished), 190.

[17] S. S. Yim, M. S. Lee, K. S. Kim, and K. B. Kim, Appl. Phys. Lett. **89**, 093115 (2006).

[18] K. S. Seol, S. J. Choi, J. Y. Choi, E. J. Jang, B. K. Kim, S. J. Park, D. G. Cha, I. Y. Song, J. B. Park, and Y. Park, Appl. Phys. Lett. **89**, 083109 (2006).

[19] S. Choi, S. S. Kim, M. Chang, H. Hwang, S. Jeon, and C. Kim, Appl. Phys. Lett. **86**, 123110 (2005).

[20] S. Maikap, P. J. Tzeng, S. S. Tseng, C. H. Lin, H. Y. Lee, C. C. Wang, L. S. Lee, T. C. Tien, S. C. Lo, P. W. Li, and M. J. Tsai, Proceedings of the 2006 International Electron Devices and Materials Symposia (IEDMS), Taiwan (unpublished), 85.

[21] S. Maikap, T. Y. Wang, H. Y. Lee, S. S. Tzeng, P. J. Tzeng, C. C. Wang, C. H. Lin, T. C. Tien, L. S. Lee, P. W. Li, J. R. Yang, and M. J. Tsai, Int. J. Nanomanufacturing (in press).